EJN fens European Journal of Neuroscience

European Journal of Neuroscience, Vol. 31, pp. 788–796, 2010 doi:10.1111/j.1460-9568.2010.07116.x

MOLECULAR AND DEVELOPMENTAL NEUROSCIENCE

β-Amyloid activates presynaptic α7 nicotinic acetylcholine receptors reconstituted into a model nerve cell system: involvement of lipid rafts

Ghous M. Khan,[1,*] Mei Tong,[1,2] Michelle Jhun,[2,3] Komal Arora[2] and Robert A. Nichols[2]
[1]Department of Pharmacology & Physiology, Drexel University College of Medicine, Philadelphia, PA 19102, USA
[2]Department of Cell and Molecular Biology, University of Hawai'i at Manoa, Honolulu, HI 96813, USA
[3]Molecular Bioscience and Bioengineering Program, University of Hawai'i at Manoa, Honolulu, HI 96813, USA

Keywords: Alzheimer's disease, beta amyloid, calcium imaging, nicotinic acetylcholine receptor, presynaptic receptor

Abstract

Beta amyloid (Aβ) plays a central role in the pathogenesis of Alzheimer's disease. Aβ is the major constituent of senile plaques, but there is a significant presence of Aβ in the brain in soluble forms. The results of functional studies indicate that soluble Aβ interacts with the α7 nicotinic acetylcholine receptor (nAChR) complex with apparent high affinity. However, conflicting data exist as to the nature of the Aβ–α7 nAChR interaction, and whether it is the result of specific binding. Moreover, both agonist-like and antagonist-like effects have been reported. In particular, agonist-like effects have been observed for presynaptic nAChRs. Here, we demonstrate $A\beta_{1\text{-}42}$-evoked stimulatory changes in presynaptic Ca^{2+} level via exogenous α7 nAChRs expressed in the axonal varicosities of differentiated hybrid neuroblastoma NG108-15 cells as a model, presynaptic system. The $A\beta_{1\text{-}42}$-evoked responses were concentration-dependent and were sensitive to the highly selective α7 nAChR antagonist α-bungarotoxin. Voltage-gated Ca^{2+} channels and internal Ca^{2+} stores were both involved in $A\beta_{1\text{-}42}$-evoked increases in presynaptic Ca^{2+} following activation of α7 nAChRs. In addition, disruption of lipid rafts by cholesterol depletion led to substantially attenuated responses to $A\beta_{1\text{-}42}$, whereas responses to nicotine were largely intact. These results directly implicate the nicotinic receptor complex as a target for the agonist-like action of pico- to nanomolar concentrations of soluble $A\beta_{1\text{-}42}$ on the presynaptic nerve terminal, including the possible involvement of receptor-associated lipid rafts. This interaction probably plays an important neuromodulatory role in synaptic dynamics.

Introduction

Beta amyloid (Aβ) has been proposed to be a key player in the development of Alzheimer's disease (Selkoe, 2002; Selkoe & Schenk, 2003). Aβ is visible as the primary component of senile plaques in the brains of Alzheimer's patients. Aβ is also significantly present in the brain in soluble form, and, in this state, was found to interact with α7 nicotinic acetylcholine receptors (α7 nAChRs) with apparent high affinity (Wang *et al.*, 2000a,b), resulting in functional regulation (Dineley *et al.*, 2001; Liu *et al.*, 2001; Pettit *et al.*, 2001).

There is, however, conflicting evidence as to the nature of the Aβ–α7 nAChR interaction. Agonist-like effects have been observed for presynaptic nAChRs. Picomolar concentrations of $A\beta_{1\text{-}42}$ were found to directly evoke sustained increases in presynaptic Ca^{2+} level in isolated presynaptic nerve endings (Dougherty *et al.*, 2003) in a manner largely dependent upon the presence of nAChRs (Mehta *et al.*, 2009). Relatively low concentrations of $A\beta_{1\text{-}42}$ elicited were also found to increase the overflow of dopamine in prefrontal cortex in the presence of tetrodotoxin (TTX), and this stimulatory effect was sensitive to antagonists of α7 nAChRs and was lost in α7 null mutant mice (Wu *et al.*, 2007). Interestingly, Aβ was also found to stimulate tau protein phosphorylation via α7 nAChRs (Wang *et al.*, 2003). On the other hand, Aβ peptides were shown to inhibit α7 nAChRs on rat hippocampal neurons in culture (Liu *et al.*, 2001) and slices (Pettit *et al.*, 2001). Aβ was also found to inhibit nAChR-mediated Ca^{2+} influx in synaptosomes (Lee & Wang, 2003; Wang *et al.*, 2009). Interaction of $A\beta_{1\text{-}42}$ with α7 nAChRs was found to facilitate Aβ internalization (Nagele *et al.*, 2002). Finally, a recent study reports a stimulatory effect of picomolar Aβ via presynaptic α7 nAChRs on long-term potentiation in the Schaffer collateral pathway of hippocampal slices, whereas an inhibitory effect was observed with high nanomolar Aβ in a manner independent of nAChRs (Puzzo *et al.*, 2008). These findings, derived from the same system, demonstrate that the stimulatory and inhibitory effects of Aβ are concentration-dependent.

By contrast, a rigorous examination of Aβ interaction with α7 nAChRs failed to reveal specific binding of the peptide to the receptor, nor did Aβ affect ligand interactions with α7 nAChRs (Small *et al.*, 2007). The major target for Aβ was found to be membrane lipids, with the main binding energy probably the result of the interaction of

Correspondence: Dr R. A. Nichols, as above.
E-mail: robert.nichols@hawaii.edu

**Present address*: College of Pharmacy, University of Appalachia, Oakwood, VA 24631, USA.

Received 24 April 2009, revised 9 December 2009, accepted 21 December 2009

hydrophobic domains on Aβ for the membrane. Thus, the definitive nature of the interaction between α7 nAChRs and Aβ remain to be defined. Furthermore, the role of an interaction of Aβ with the membrane, and its resultant impact on nAChR regulation, also needs to be clarified. This study was therefore undertaken to study functional changes in presynaptic Ca^{2+} occurring in response to Aβ activation in a model neuronal system expressing exogenous presynaptic α7 nAChRs. In addition, a potential role for lipid rafts in Aβ-evoked presynaptic Ca^{2+} responses was assessed.

Materials and methods

Cell culture and expression of exogenous α7 nAChRs

NG108-15 cells (from Dr. William Atchison, Michigan State University) were cultured in high-glucose Dulbecco's modified Eagle's medium (DMEM) containing 15% fetal bovine serum (FBS), 0.1 mM hypoxanthine, 1 μM aminopterin and 16 μM thymidine in the presence of 5% CO_2 at 37°C (Nelson *et al.*, 1976). Cells were plated at low density onto Cell-Tak-coated coverslips in 35-mm dishes and then differentiated with dibutyryl-cyclic AMP (1 mM) (Sigma-Aldrich) in DMEM with 1% FBS. After 2–3 days, a pcDNA3.1 construct containing the mouse α7 nAChR sequence (courtesy of Dr Jerry Stitzel, University of Colorado) was transfected into differentiated cells using the transfectant reagent FuGENE 6 (Roche Diagnostics), obtaining typically > 80% transfection efficiency as previously described (Nichols *et al.*, 2007). As primary control, empty pcDNA3.1 constructs were transfected as well. Mock-transfected control cells were incubated only with the transfection reagent.

Confocal imaging

After 1–2 days, the transfected, differentiated cells were loaded with fluorescent Ca^{2+} indicator dye Fluo-4/AM (Invitrogen) at 5 μM in HEPES-buffered saline (HBS) containing (in mM) 142 NaCl, 2.4 KCl, 1.2 K_2PO_4, 1 $MgCl_2$, 1 $CaCl_2$, 5 D-glucose, pH 7.4, and saturated with O_2 at 37°C for 1–1.5 h in preparation for confocal imaging, as described (Nichols *et al.*, 2007). Cells were mounted in a rapid-exchange Warner perfusion system (36 μL) for confocal imaging using either a Nikon Diaphot microscope attached to a Nikon PCM 2000 or a Zeiss Axiovert 200M attached to a Zeiss LSM 5 Pascal imaging system. Perfusion with HBS containing 100 nM TTX at 3–5 mL/min was started. Atropine (1 μM) was added to the HBS as required. Imaging was commenced (excitation: 488nm; emission: 515–565 nm band-pass; 40×/1.3 epifluorescence, oil-immersion Plan-Neofluar objective) and after obtaining a baseline series of four images, stimulatory and/or inhibitory agents were applied by rapid switching between manifolds on the perfusion system. Images were typically collected at 2- or 5-s intervals unless otherwise noted.

Cholesterol depletion

Depletion of membrane cholesterol to disrupt lipid rafts in the differentiated NG108-15 cells was performed using methyl-β-cyclodextrin (Zidovetzki & Levitan, 2007). In brief, cultures on Cell-Tak-coated coverslips in 35-mm dishes were washed with HBS and then incubated with 0.5 or 15 mM methyl-β-cyclodextrin (CTD, Inc.) in HBS for 15 min at room temperature (Barrantes, 2007). For 15 mM methyl-β-cyclodextrin, $\sim$ 50% of cell cholesterol will be extracted (Zidovetzki & Levitan, 2007), preferentially from the plasma membrane, which is estimated to have roughly half of the total cellular cholesterol (Warnock *et al.*, 1993), without substantial effect on surface nAChR expression (Barrantes, 2007). Cultures were rapidly washed three times with HBS to remove the methyl-β-cyclodextrin. To assess disruption of lipid rafts, cultures were fixed with 4% paraformaldehyde in HBS at room temperature for 30 min, rinsed with phosphate-buffered saline (PBS), and then stained for 15 min with $Alexa^{488}$-conjugated recombinant Cholera Toxin subunit B using the Vybrant staining kit (Invitrogen). The labeled Cholera Toxin subunit B selectively stains GM1 ganglioside, a key lipid raft component. To assess the effect of disruption of lipid rafts on Aβ-evoked Ca^{2+} responses, the cultures were preloaded with Fluo-4, as described previously, prior to treatment with methyl-β-cyclodextrin, briefly washed with HBS and then imaged using confocal microscopy as described.

Immunostaining

Cell cultures were fixed with 4% paraformaldehyde in HBS at room temperature for 30 min, rinsed with PBS and then permeabilized with 0.1% Triton X-100 in PBS for 15 min. The cultures were then incubated in PBS containing 5% bovine serum albumin, 10% normal goat serum and 0.1% TritonX-100 for 30 min to block non-specific binding. Affinity-purified anti-α7 nAChR antibody (1 : 100; Chemicon) was then added to the cultures and incubated for 60 min at room temperature. The cultures were then washed with 10% goat serum plus 0.1% TritonX-100 in PBS, and incubated with the FITC-conjugated goat anti-rabbit IgG (1 : 200; Jackson Immunoresearch) as secondary antibody, for 60 min at room temperature. Background staining was assessed using the secondary antibody alone (Nayak *et al.*, 2000). The cultures were finally washed with 10% normal goat serum and PBS, plated onto glass microscope slides and sealed for imaging via confocal microscopy.

Chemicals

Cell Tak was from BD Biosciences (Bedford, MA, USA). Nicotine tartrate citrate, acetylcholine chloride, choline chloride, caffeine, nitrendipine and atropine chloride were all purchased from Sigma-Aldrich. Nicotine, acetylcholine, choline and caffeine solutions were freshly prepared. A$\beta_{1\text{-}42}$ was purchased from BACHEM (King of Prussia, PA, USA), while ω-conotoxin GVIA, TTX and α-BgTx were from Calbiochem (La Jolla, CA, USA). Methyl-β-cyclodextrin was from Cyclodextrin Technologies (CTD, Inc., Gainesville, FL, USA). The Vybrant Lipid Raft staining kit was from Invitrogen (Carlsbad, CA, USA). All drugs, except A$\beta_{1\text{-}42}$ and nitrendipine, were made into solutions in HBS. Stock nitrendipine (20 mM) was dissolved in dimethyl sulfoxide. Stock solutions of A$\beta_{1\text{-}42}$ (1 mM) were made in water with vigorous vortexing (Dougherty *et al.*, 2003). Native and Western immunoblot analysis of nanomolar concentration of A$\beta_{1\text{-}42}$ in HBS demonstrated the presence of several oligomeric forms, with little evidence of monomer under native conditions (see Fig. S1), consistent with prior analyses (Bell *et al.*, 2004).

Data analysis and statistics

The fluorescent intensities associated with individual varicosities were determined from digitized images by a blind observer using MetaMorph image analysis software and were expressed as normalized values (F/F_0, where F_0 is the fluorescence intensity at time zero). All time series were corrected for photobleaching (typically < 3%). Averaged data are presented as means ± SEM, where *n* refers to the

number of (pooled) varicosities examined. Peak amplitudes (as F/F_0) were determined from averaged maximum plateau values. Peak amplitudes were compared using one-way ANOVA with Bonferroni multiple comparison *post hoc* test or two-tailed Student's *t*-test for two groups, using GRAPHPAD INSTAT 3. Significance was indicated when P was minimally < 0.05.

Results

Nicotinic agonists elicit dose-dependent Ca^{2+} responses in NG108-15 neuritic presynaptic-like varicosities expressing α7 nAChRs

Differentiated NG108-15 cells elaborate long, branched axonal processes containing large varicosities (~5–15 μM) that are fully capable of forming synapses with an appropriate target (Nelson *et al.*, 1976), but do not synapse on each other. In the absence of synapse formation, the axonal varicosities otherwise display features of a presynaptic element (Han *et al.*, 1991), including synaptic vesicles capable of supporting neurotransmitter release (McGee *et al.*, 1978) and voltage-gated Ca^{2+} channels (VGCCs) typical of presynaptic terminals (Lukyanetz *et al.*, 1998), and thus permit assessment of presynaptic regulation in discretely identifiable structures. There are equivalent structures existing in the central nervous system, as axonal varicosities proposed to release neurotransmitter at a distance (so-called volume transmission) from postsynaptic targets have been noted in the brain for several neurotransmitter systems (e.g. Umbriaco *et al.*, 1994). A propos of the present study, these cells (and their varicosities) do not express functional nicotinic receptors, but do express 5-HT_3 receptors on their cell bodies (Yakel *et al.*, 1991) and axonal varicosities (Ronde & Nichols, 2001). These receptors are both members of the ligand-gated ion channel superfamily. Hence, the cells were predicted to have all of the necessary components for their expression and could thus serve as a neuronal system for 'reconstituting' presynaptic nicotinic receptors via exogenous expression.

The presence of α7 nAChRs in axonal varicosities (arrows) of differentiated NG108-15 cells transfected with pcDNA3.1 vector containing the mouse α7 nAChR sequence (Fig. 1B and C) was detected by immunocytochemistry using a recently developed anti-mouse α7 nAChR antibody (Chemicon) and visualized via confocal imaging. The background fluorescence resulting from immunostaining of differentiated NG108-15 cells transfected with empty vector using the same anti-mouse α7 nAChR antibody is shown for comparison in Fig. 1A.

The effects of nAChR agonists such as nicotine, acetylcholine and choline were tested on the axonal varicosities of NG108-15 cells transfected with murine α7 cDNA, measuring Ca^{2+} responses using confocal imaging typically 24-48 h after transfection. Increasing concentrations of the nAChR agonist nicotine (500 nM, 1 μM and 10 μM) were applied in the presence of TTX (100 nM to block regenerative responses), and induced rapid-onset, sustained increases in [Ca^{2+}] in the neuritic varicosities, as detected by relative increases in fluorescence signal (Fig. 2A). To varying degrees, nicotine also induced Ca^{2+} responses in cell bodies. Both 1 and 10 μM nicotine (Fig. 2B) produced maximum responses in the varicosities (2.86 ± 0.33 F/F_0, $F_{4,38} = 38$, $P < 0.001$ and 2.96 ± 0.39 F/F_0, $F_{4,38} = 37$, $P < 0.001$, respectively, compared with control), which were significantly more pronounced than that of 500 nM nicotine (1.58 ± 0.01 F/F_0, $P > 0.05$ vs. control). Responses to all the concentrations of nicotine used in the experiment were completely blocked by perfusion with α-bungarotoxin (α-BgTx; 30 nM) (Fig. 2B, 1.24 ± 0.02 F/F_0 for 1 μM nicotine, $P > 0.05$ vs. control), a highly selective α7 nAChRs receptor antagonist. Extending the length of perfusion of nicotine (10 μM) for 7 min evoked sustained increases in Ca^{2+} response that peaked around 3 min and then gradually returned to baseline (Fig. S2). No response was observed to nicotine in mock-transfected preparations (Figs 2B and S2).

The specific α7 nAChR agonist choline also evoked dose-dependent Ca^{2+} responses in axonal varicosities expressing α7 nAChRs (Fig. 2C, 1.82 ± 0.08 F/F_0, $F_{3,36} = 86$, $P < 0.001$ and 1.42 ± 0.06 F/F_0, $F_{3,36} = 27$, $P < 0.001$ for 500 and 50 μM choline, respectively, compared with control). Similarly, the AChR agonist acetylcholine, applied in the presence of atropine to isolate its nicotinic action, evoked concentration-dependent Ca^{2+} responses (Fig. 2D, 1.36 ± 0.05 F/F_0, $F_{3,24} = 17$, $P < 0.01$ and 1.50 ± 0.50 F/F_0, $F_{3,24} = 34.7$, $P < 0.001$ for 1 and 5 mM acetylcholine, respectively, compared with control), although they were not as consistently robust as those seen with nicotine or choline. Responses to both choline and acetylcholine were blocked by α-BgTx (50 nM; 1.066 ± 0.02 F/F_0, $P > 0.05$ vs. control and 1.12 ± 0.02 F/F_0, $P > 0.05$ vs. control, respectively).

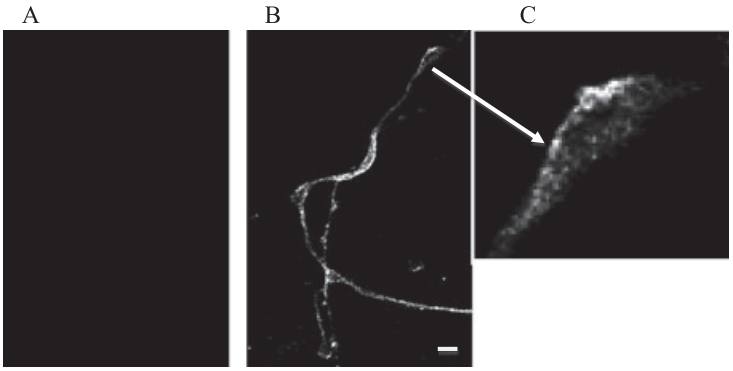

FIG. 1. Representative images demonstrating the presence of α7 nAChR in axonal varicosities (e.g. arrow) of differentiated NG108-15 cells transfected with pcDNA3.1 vector containing the mouse α7 nAChR sequence (B), as detected by immunocytochemistry using a recently developed anti-mouse α7 nAChR antibody (Chemicon) and visualized with confocal imaging. Panel A shows the background fluorescence resulting from immunocytochemistry with the same anti-mouse α7 nAChR antibody applied to differentiated NG108-15 cells transfected with empty pcDNA3.1 vector (A). Panel C shows a magnified view of an immunopositive varicosity (B, upper right). Scale bar = 10 μm.

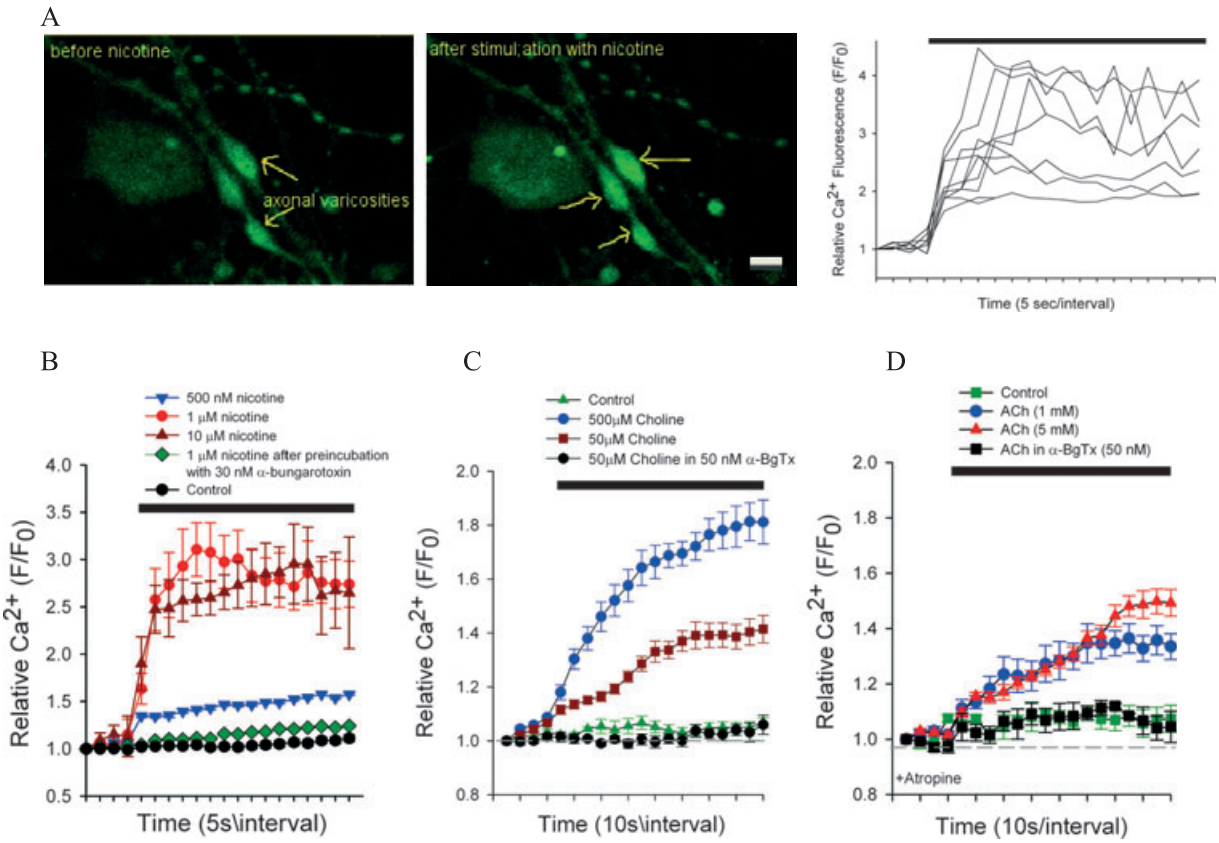

FIG. 2. Nicotinic agonist-evoked increases in $[Ca^{2+}]_i$ in axonal varicosities of NG108-15 cells transfected with mouse α7 nAChR. (A) Representative confocal image sequence (left) and individual Ca^{2+} responses (right) to 1 μM nicotine (bar) in NG108-15 varicosities expressing α7 nAChRs. Scale bar = 10 μm. Averaged time series of changes in Ca^{2+} in varicosities in response to increasing concentrations of (B) nicotine (500 nM, $n = 10$; 1 μM, $n = 8$; 10 μM, $n = 6$), as compared with 1 μM nicotine applied to mock-transfected cultures (control, $n = 6$); (C) choline (500 μM; $n = 7$; 50 μM; $n = 14$), a specific α7 nAChR agonist, as compared with control cultures ($n = 6$); (D) acetylcholine (ACh: 5 mM, $n = 8$; 1 mM, $n = 9$), as compared with control ($n = 6$). For all agonists, pretreatment with α-BgTx (30 or 50 nM) for 30 min completely blocked the agonist-evoked Ca^{2+} responses (1 μM nicotine, $n = 13$; 50 μM choline, $n = 13$; ACh, $n = 5$). For acetylcholine, atropine (1 μM) was added to block muscarinic AChRs. Ca^{2+} responses were assessed via confocal imaging following loading with the Ca^{2+} -sensitive fluorescent dye Fluo-4.

$A\beta_{1\text{-}42}$ induces Ca^{2+} responses in NG108-15 neuritic varicosities expressing α7 nAChRs

Previous work employing functional approaches suggested that the beta amyloid peptide regulates α7 nAChRs (Liu *et al.*, 2001; Pettit *et al.*, 2001; Dougherty *et al.*, 2003; Wu *et al.*, 2007; Puzzo *et al.*, 2008; Mehta *et al.*, 2009), but none of the studies demonstrated definitively a direct interaction, and pharmacological inhibition of Aβ-regulated responses using nicotinic antagonists was often partial. Moreover, specific binding of Aβ to nAChRs has been questioned (Small *et al.*, 2007). Using NG108-15 cells expressing exogenous α7 nAChR, we tested the acute effect of soluble $A\beta_{1\text{-}42}$. Soluble $A\beta_{1\text{-}42}$ (100 nM) evoked sharp and sustained responses (Fig. 3, 2.89 ± 0.35 F/F_0, $F_{2,25} = 18$, $P < 0.001$ vs. control reverse peptide), similar to those obtained using nicotine. The responses were nearly completely blocked by α-BgTx (Fig. 3B, $P > 0.05$ vs. control peptide). Soluble $A\beta_{1\text{-}42}$ evoked no response in mock-transfected varicosities and/or cell bodies. The small, slow increase in Ca^{2+} observed with the reverse peptide $A\beta_{42\text{-}1}$ in NG108-15 neuritic varicosities expressing α7 nAChRs (Fig. 3B) may indicate a direct membrane effect of the hydrophobic elements in Aβ (Small *et al.*, 2007). However, the block by α-BgTx would indicate an absence of a non-specific membrane effect by Aβ when the receptor is blocked. Extending the length of perfusion of $A\beta_{1\text{-}42}$ (100 nM) for 7 min evoked sustained increases in Ca^{2+} response that peaked around 3 min and then gradually returned to baseline (Fig. S3), similar to that observed for nicotine. The $A\beta_{1\text{-}42}$-evoked Ca^{2+} responses were concentration-dependent (Fig. 3C), with an EC_{50} between 1 and 100 nM. Addition of nicotine (500 nM) at the peak of the $A\beta_{1\text{-}42}$-evoked Ca^{2+} response had no impact (Fig. 3D), consistent with prior evidence (Dougherty *et al.*, 2003; Mehta *et al.*, 2009) showing that activation by Aβ occludes the response to subsequent co-application of nicotine.

Nature of Ca^{2+} responses to $A\beta_{1\text{-}42}$

In NG108-15 axonal varicosities, $5\text{-}HT_3$ receptor agonist-evoked Ca^{2+} responses were previously shown to depend on VGCCs and Ca^{2+} stores (Rondé & Nichols, 2001), indicating that the receptors trigger depolarization via Na^+ influx, opening VGCCs, and Ca^{2+} -induced Ca^{2+} release (CICR) subsequent to the resultant Ca^{2+} influx. Because α7 nAChR activation will also result in substantial Ca^{2+} influx and depolarization (Role & Berg, 1996), it was important to examine the roles of VGCCs and internal Ca^{2+} stores in $A\beta_{1\text{-}42}$-evoked Ca^{2+} responses via nAChRs in NG108-15 varicosities. To test the role of VGCCs in $A\beta_{1\text{-}42}$-evoked Ca^{2+} responses, we co-applied two Ca^{2+} channel antagonists, nitrendipine (20 μM), an L-type VGCC blocker, and ω-conotoxin GVIA (500 nM), an N-type VGCC blocker, which block depolarization-induced Ca^{2+} responses (see Rondé & Nichols, 2001). The Ca^{2+} channel blockers significantly inhibited Aβ-evoked responses in axonal varicosities of NG108-15 cells expressing α7

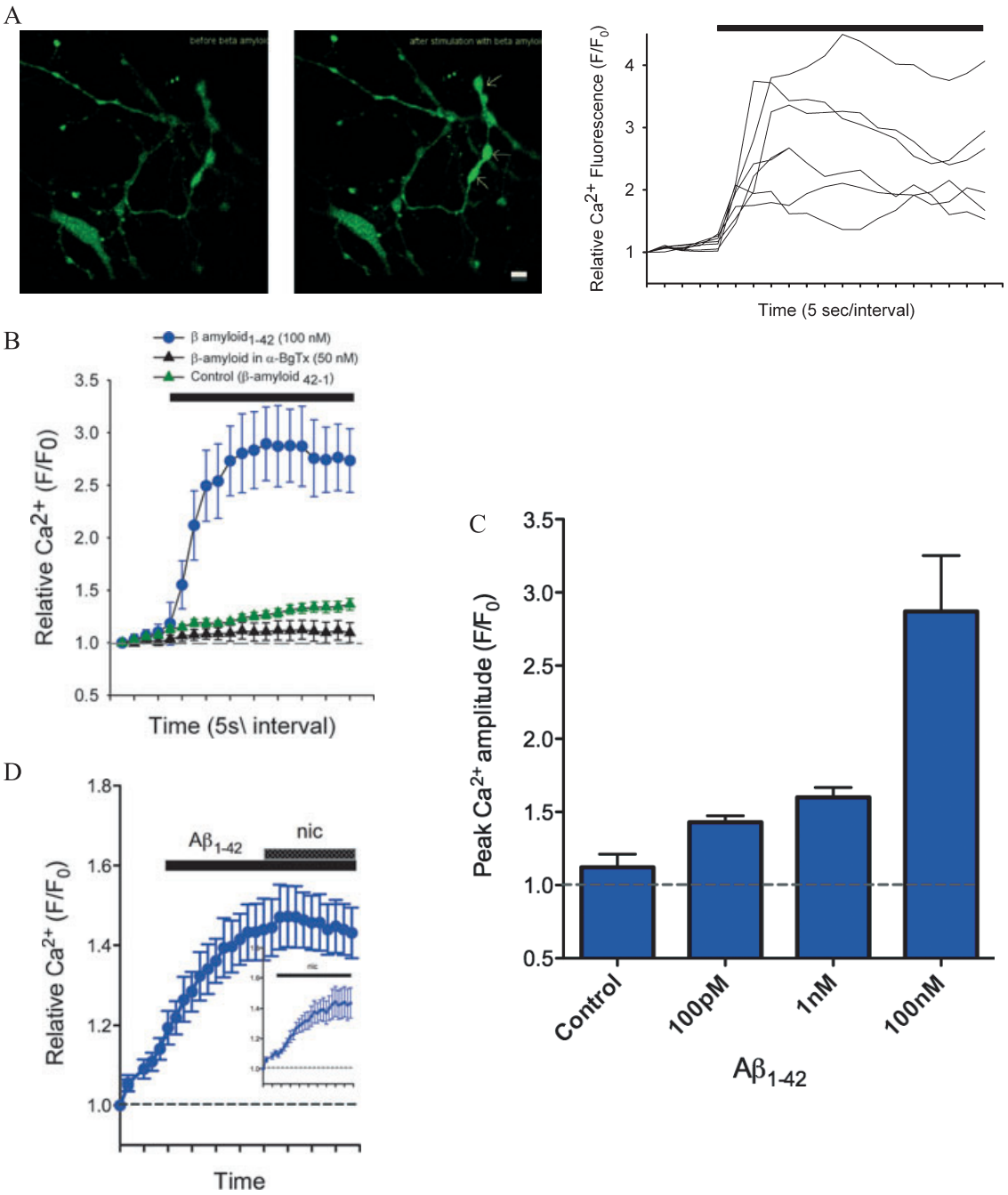

FIG. 3. Aβ-evoked increases in $[Ca^{2+}]_i$ in axonal varicosities of NG108-15 cells transfected with mouse α7 nAChR. (A) Representative confocal image sequence (left) and individual Ca^{2+} responses (right) to 100 nM A$\beta_{1\text{-}42}$ (bar) in NG108-15 varicosities expressing α7 nAChRs. Scale bar = 10 μm. (B) Averaged time series of changes in Ca^{2+} in varicosities in response to 100 nM A$\beta_{1\text{-}42}$ in the absence (n = 13) or presence of 50 nM α-BgTx (30-min pretreatment; n = 9). For comparison, the effect of reverse sequence peptide A$\beta_{42\text{-}1}$ was assessed (control; n = 6). There was no effect of A$\beta_{1\text{-}42}$ on mock-transfected or empty vector-transfected cultures (not shown). (C) Histogram of average peak amplitudes of Ca^{2+} responses to increasing concentrations of A$\beta_{1\text{-}42}$ (Control, n = 6; 100 pM, n = 7; 1 nM, n = 6; 100 nM, n = 9, $F_{3,24}$ = 23.8, $P < 0.001$). Ca^{2+} responses were assessed via confocal imaging following loading with the Ca^{2+} -sensitive fluorescent dye Fluo-4. (D) Averaged time series of changes in Ca^{2+} in varicosities in response to 100 nM A$\beta_{1\text{-}42}$ followed by co-administration of 500 nM nicotine, where indicated (n = 9). Inset shows effect of stimulation with nicotine alone in a sister culture (n = 9).

nAChRs (Fig. 4A, 1.2 ± 0.05 F/F_0, $F_{2,25}$ = 24, $P < 0.001$ vs. control response to Aβ). The small increase in the presence of the VGCC blockers is probably the result of Ca^{2+} influx directly via the receptor channel (Rondé & Nichols, 2001).

Ca^{2+} influx through presynaptic nAChRs was found to lead to mobilization of Ca^{2+} from internal Ca^{2+} stores via CICR in hippocampal terminals (Sharma & Vijayaraghavan, 2003; La Magueresse & Cherubini, 2007; Sharma *et al.*, 2008) and glutamatergic prefrontal cortical terminals (Dickinson *et al.*, 2008), contributing to the modulation of neurotransmitter release. To test this pathway, intracellular Ca^{2+} stores were first depleted using millimolar caffeine in the presence of EGTA and then perfused with A$\beta_{1\text{-}42}$. No significant responses were elicited by A$\beta_{1\text{-}42}$ in Ca^{2+} store-depleted varicosities (Fig. 4A, $F_{2,25}$ = 37, $P < 0.001$ vs. control

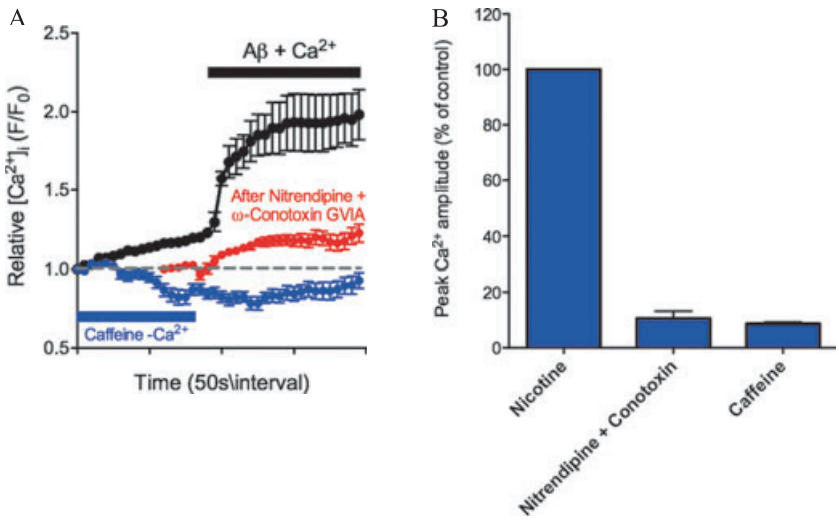

FIG. 4. Aβ-evoked increases in $[Ca^{2+}]_i$ in axonal varicosities of NG108-15 cells transfected with mouse α7 nAChR depend on VGCCs and CICR. (A) Averaged time series of changes in Ca^{2+} in varicosities in response to 100 nM $A\beta_{1-42}$ in the presence of 20 μM nitrendipine and 500 nM ω-conotoxin GVIA (10-min pretreatment; $n = 16$) compared with prior depletion of Ca^{2+} stores using 10 mM caffeine in the absence of external Ca^{2+} (blue bar) $n = 6$. (B) Effect of pretreatment with 20 μM nitrendipine and 500 nM ω-conotoxin GVIA ($n = 5$) compared with prior depletion of Ca^{2+} stores using 10 mM caffeine ($n = 6$) on nicotine-induced Ca^{2+} responses (peak amplitudes normalized to control nicotine response, $n = 8$; see Fig. 2).

response to Aβ). Similar blockade by the Ca^{2+} channel antagonists ($F_{2,17} = 15.2$, $P < 0.01$) or caffeine-induced store depletion ($F_{2,17} = 14.6$, $P < 0.01$) was found for nicotine-induced Ca^{2+} responses (Fig. 4B). In summary, these results indicate that the α7 nAChR activation upon Aβ application to the NG108-15 varicosities results in Ca^{2+} influx via VGCCs, which, together with Ca^{2+} influx via the receptor channel, triggers CICR.

Lipid raft disruption abolished Aβ-evoked responses

In view of the noted interaction of Aβ with membrane lipids (Small *et al.*, 2007), particularly GM1 ganglioside (Kakio *et al.*, 2002) and the noted small but detectable effect of $A\beta_{42-1}$ (see Fig. 3B), we tested whether disruption of lipid rafts, proposed to associate with α7 nAChRs (Brusés *et al.*, 2001), had any impact on $A\beta_{1-42}$-evoked Ca^{2+} responses via nAChRs in NG108-15 varicosities. Prior application of 0.5 or 15 mM methyl-β-cyclodextrin for 15 min to deplete membrane cholesterol and hence disrupt associated lipid rafts (Fig. 5A, right) attenuated $A\beta_{1-42}$-evoked responses in α7 nAChR-transfected varicosities (Fig. 5A, left, $F_{2,16} = 41$, $P < 0.001$ for 15 mM cyclodextrin vs. control response to Aβ). The higher concentration (15 mM) of methyl-β-cyclodextrin has been shown to substantially deplete the membrane of cholesterol, whereas the lower concentration (0.5 mM) will only partially deplete the membrane (Zidovetzki & Levitan, 2007), and the results are generally consistent with this difference. Cholesterol depletion with 15 mM methyl-β-cyclodextrin only partially attenuated nicotine-induced responses (Fig. 5B, left; nicotine: 68%, as compared with initial stimulation, $P = 0.002$, two-tailed unpaired *t*-test), indicating that nicotine's interaction with the receptor is largely intact. Interestingly, ACh-induced Ca^{2+} responses were substantially reduced, but not eliminated, following cholesterol depletion (Fig. 5B, right; ACh: 39%, as compared with initial stimulation, $P = 0.002$, two-tailed unpaired *t*-test). That robust responses to K^+-depolarization remained after treatment of the cells with methyl-β-cyclodextrin verified the viability of the preparations (Fig. 5B). Disruption of lipid rafts by methyl-β-cyclodextrin did not appear to alter the overall expression of α7 nAChRs (Fig. 5C). These results suggest an important role for associated lipids in the agonist-like effect of Aβ on presynaptic α7 nAChRs.

Discussion

Soluble Aβ can aggregate into soluble prefibrillar intermediates, largely as low-molecular weight oligomers (Walsh & Selkoe, 2007). Soluble oligomers are proposed to play significant roles in the pathogenesis of Alzheimer's disease (Selkoe, 2008) and their levels have been found to strongly correlate with the neurodegenerative process in patients with Alzheimer's disease (McLean *et al.*, 1999). We report here the acute stimulatory effects of soluble Aβ in the presynaptic-like axonal varicosities of NG108-15 cells expressing α7 nAChRs, comparable with Ca^{2+} responses evoked by nicotinic agonists. These effects were assessed as changes in Ca^{2+} levels in the axonal varicosities, as the regulation of presynaptic Ca^{2+} is integral to synaptic function. The Ca^{2+} responses to soluble $A\beta_{1-42}$ applied to varicosities expressing α7 nAChRs were blocked by α-BgTx, a potent and highly selective antagonist of α7 nAChRs. In addition, the $A\beta_{1-42}$-elicited responses were not observed in axonal varicosities of mock-transfected cells. Together, these results confirm a direct interaction of Aβ with presynaptic α7 nAChRs. To our knowledge, this is the first instance of a putative receptor target for pico- to nanomolar Aβ, identified in *ex vivo* and *in vivo* studies of presynaptic terminals (Dougherty *et al.*, 2003; Wu *et al.*, 2007; Puzzo *et al.*, 2008; Abbott *et al.*, 2008; Mehta *et al.*, 2009; Wang *et al.*, 2009), being 'reconstituted' in a neuronal culture system. Other studies describe effects of Aβ on exogenous nAChRs expressed *in vitro*, but the systems used did not reconstitute the equivalent environment, here the presynaptic nerve terminal.

The pronounced reduction in Aβ-evoked Ca^{2+} responses following the application of Ca^{2+} channel blockers to the differentiated cultures suggest that presynaptic VGCCs are a major component in the overall Ca^{2+} entry in cases where nAChRs evoke significant changes in membrane potential. In addition, the loss of Aβ-evoked responses in varicosities in which internal Ca^{2+} stores were depleted suggests that CICR may play a dominant role in Aβ-triggered presynaptic

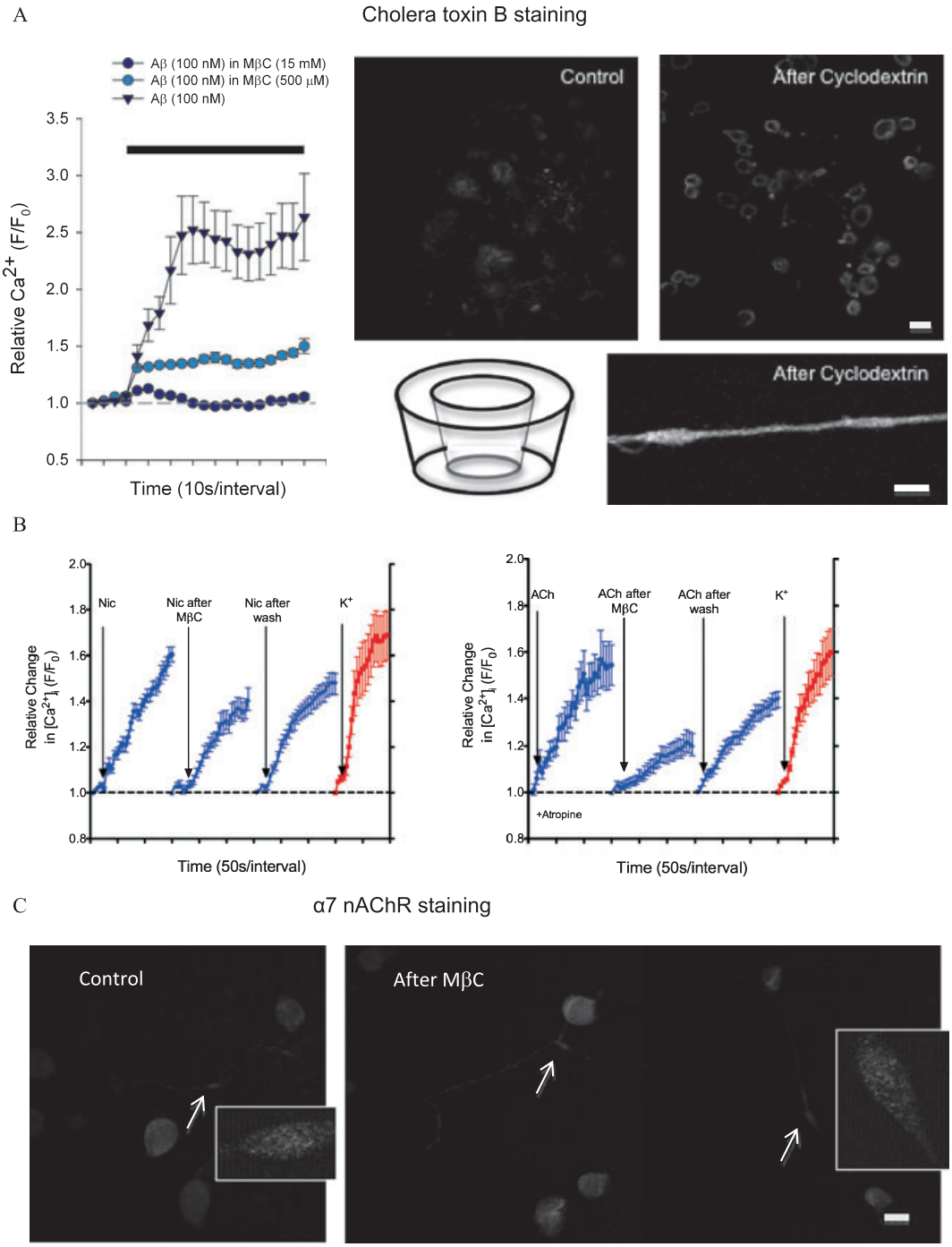

FIG. 5. Cholesterol depletion via methyl-β-cyclodextrin to disrupt lipid rafts abolishes A$\beta_{1\text{-}42}$- evoked responses in α7 nAChR-transfected varicosities in NG108-15 cells. (A) Left: averaged time series of Ca^{2+} responses to 100 nM A$\beta_{1\text{-}42}$ in varicosities transfected with α7 nAChR pretreated (closed circles) or not (control: triangles) with methyl-β-cyclodextrin at 0.5 mM (n = 6) or 15 mM (n = 7) for 15 min (Barrantes, 2007). To maintain identical experimental conditions, the untreated (control) cultures (n = 6) were pre-incubated for the same length of time in HBS before perfusing with A$\beta_{1\text{-}42}$. Right: confocal micrographs showing lipid raft disruption after treatment with methyl-β-cyclodextrin schematic to deplete membrane cholesterol, using Alexa^{488}-conjugated Cholera Toxin B staining (Vybrant Lipid Raft kit) for GM1 ganglioside, a key lipid raft component. Lipid rafts appeared as patchy staining on control cells, shifting to uniform, diffuse staining after cholesterol depletion. Upper sequence: scale bar = 30 μm; lower micrograph: scale bar = 10 μm. (B) Averaged time series of Ca^{2+} responses to 1 μM nicotine (left sequence; n = 18) or 0.5 μM ACh in the presence of 1 μM atropine (right sequence; n = 14) in varicosities transfected with α7 nAChR following sequential treatment with HBS, methyl-β-cyclodextrin at 15 mM for 15 min, and an additional 10-min wash with HBS followed by stimulation with nicotine or ACh (blue curves). Each sequence was followed by stimulation with 30 mM KCl (red curves). Preparations were washed for 5–10 min between each stimulation. (C) Immunostaining NG108-15 cells and varicosities (arrows) for α7 nAChRs before (control) and after (MβC) treatment (two fields). Scale bar = 30 μm.

responses. Together, these data show that the activation of presynaptic α7 nAChRs by pico- to nanomolar Aβ has a two-component Ca^{2+} entry into the varicosities, similar to that observed for nicotinic agonist activation of the receptor. The first is from a direct permeation of Ca^{2+} via the nAChR channel, while the second results from entry via VGCCs opened in response to simultaneous nAChR-evoked

membrane depolarization. In response to this Ca^{2+} entry, CICR is evoked, resulting in a substantial amplification and prolongation of the signal.

Ionic currents mediated by α7 nAChRs expressed in cell bodies typically display rapid desensitization (Role & Berg, 1996). In contrast, presynaptic nicotinic receptor activation has been found to result in a prolonged stimulatory effect (McGehee *et al.*, 1995; Gray *et al.*, 1996; Nayak *et al.*, 2001; Sharma & Vijayaraghavan, 2003) depending on the preparation (Mansvelder *et al.*, 2002; Mehta *et al.*, 2009). As noted, CICR, where it occurs, will further prolong the signal. The apparent kinetics of an agonist-like effect of A*β* on presynaptic signals also indicate a prolonged action. This effect is in sharp contrast to the effect of A*β* on nicotinic receptors expressed in cell bodies or dendrites (e.g. Liu *et al.*, 2001, 2009; Pettit *et al.*, 2001; Wu *et al.*, 2004). One possible explanation for the difference may be that A*β* rapidly induces, or stabilizes, the inactivated state of the nAChRs when expressed at postsynaptic or somatic sites, resulting in an antagonist-like action, whereas a slower rate of desensitization of presynaptic nAChRs may permit the agonist-like effect of A*β*. This possibility might be addressed, ideally, by examining ionic nicotinic currents at presynaptic and postsynaptic sites in the same system.

Regardless, the basis for the distinct behavior of presynaptic nAChRs remains to be elucidated. We have speculated that the microenvironment of the nAChR complex in the presynaptic terminal may be unique (Nayak *et al.*, 2001). Axons and terminals of neurons have been deemed to be large extensions of classical apical membranes, particularly in view of the abundant presence of lipid rafts (Tsui-Pierchala *et al.*, 2002). We thus examined whether cholesterol depletion, to disrupt lipid rafts, had an impact on A*β*-evoked presynaptic Ca^{2+} responses. Remarkably, the A*β*-evoked responses in the varicosities were dramatically attenuated following cholesterol depletion by methyl-*β*-cyclodextrin, whereas nicotine-evoked responses were largely intact. Although cholesterol depletion will also occur in non-raft membrane (Zidovetzki & Levitan, 2007), clear disruption of lipid rafts, as detected via staining for GM1 ganglioside, which is a prominent component of rafts, was observed. In view of the hydrophobic domain of A*β* (Walsh & Selkoe, 2007), derived from part of the predicted transmembrane domain of the amyloid precursor protein, we postulate that an interaction of A*β* directly with the membrane (Small *et al.*, 2007) may influence its targeting and regulation of presynaptic nAChRs. There is evidence that GM1 ganglioside interacts with A*β* (Kakio *et al.*, 2002) and thus the lipid raft microenvironment may serve to guide A*β* in its interaction with the receptor, positioning it to interact with the ligand-binding (activation) domain. In addition, a dual lipid raft–receptor interaction may also explain the apparent picomolar potency of A*β* for the nAChRs in the varicosities, as the apparent affinity of A*β* will be a power-function composite of its individual affinities for the raft/membrane and the receptor.

The precise target(s) for A*β* in the membrane, the precise form (oligomeric?) of A*β* interacting with the membrane targets, and how the membrane target(s) contributes to the targeting and/or regulation of presynaptic nAChRs remain to be determined, particularly as lipid rafts are also present in the somata. Lipid–nAChR interactions have been noted (Barrantes, 2004), as an annular shell around the transmembrane core of the receptor, and, in addition, such lipid shells may participate in mediating receptor-raft targeting (Anderson & Jacobson, 2002). The interaction of rafts with the receptor complex and the interaction of A*β* with unique components in the rafts may provide a link among the disparate receptor systems found to be regulated by soluble A*β*.

Supporting Information

Additional supporting information may be found in the online version of this article:

Fig. S1. SDS–PAGE and native gel analysis of the A*β* preparation solubilized in aqueous buffered solution.

Fig. S2. Averaged time series of Ca^{2+} responses in the varicosities of differentiated NG108-15 cells expressing exogenous α7 nAChRs or not (mock-transfected) to an extended length of perfusion (> 5 min) with nicotine (10 μM).

Fig. S3. Averaged time series of Ca^{2+} responses in the varicosities of differentiated NG108-15 cells expressing exogenous α7 nAChRs to an extended length of perfusion (> 5 min) with $A\beta_{1-42}$ (100 nM).

Please note: As a service to our authors and readers, this journal provides supporting information supplied by the authors. Such materials are peer-reviewed and may be re-organized for online delivery, but are not copy-edited or typeset by Wiley-Blackwell. Technical support issues arising from supporting information (other than missing files) should be addressed to the authors.

Acknowledgements

We thank Dr Jerry Stitzel, University of Colorado, for providing the mouse α7 nAChR sequence in the pcDNA3.1zeo expression vector. We thank Michelle Guerin for excellent technical assistance. We also thank Dr Frederick Bellinger for critical reading of the manuscript. This work was supported by grants from the American Health Assistance Foundation and the National Institute on Aging (AG21586).

Abbreviations

A*β*, beta amyloid; CICR, Ca^{2+} -induced Ca^{2+} release; HBS, HEPES-buffered saline; nAChR, nicotinic acetylcholine receptors; TTX, tetrodotoxin; VGCC, voltage-gated calcium channel; α-BgTx, α-bungarotoxin.

References

Abbott, J.J., Howlett, D.R., Francis, P.T. & Williams, R.J. (2008) $A\beta_{1-42}$ modulation of Akt phosphorylation via α7 nAChR and NMDA receptors. *Neurobiol. Aging*, **29**, 992–1001.

Anderson, R.G. & Jacobson, K. (2002) A role for lipid shells in targeting proteins to caveolae, rafts, and other lipid domains. *Science*, **296**, 1821–1825.

Barrantes, F.J. (2004) Structural basis for lipid modulation of nicotinic acetylcholine receptor function. *Brain Res. Rev.*, **47**, 71–95.

Barrantes, F.J. (2007) Cholesterol effects on nicotinic acetylcholine receptor. *J. Neurochem.*, **103**, 72–80.

Bell, K.A., O'Riordan, K.J., Sweatt, J.D. & Dineley, K.T. (2004) MAPK recruitment by *β*-amyloid in organotypic hippocampal slice cultures depends on physical state and exposure time. *J. Neurochem.*, **91**, 349–361.

Brusés, J.L., Chauvet, N. & Rutishauser, U. (2001) Membrane lipid rafts are necessary for the maintenance of the α7 nicotinic acetylcholine receptor in somatic spines of ciliary neurons. *J. Neurosci.*, **21**, 504–512.

Dickinson, J.A., Kew, J.N.C. & Wonnacott, S. (2008) Presynaptic α7 and *β*2-containing nicotinic acetylcholine receptors modulate excitatory amino acid release from rat prefrontal cortex nerve terminals via distinct cellular mechanisms. *Mol. Pharmacol.*, **74**, 348–359.

Dineley, K.T., Westerman, M., Bui, D., Bell, K., Ashe, K.H. & Sweatt, J.D. (2001) *β*-amyloid activates the mitogen-activated protein kinase cascade via hippocampal α7 nicotinic acetylcholine receptors: in vitro and in vivo mechanisms related to Alzheimer's disease. *J. Neurosci.*, **21**, 4125–4133.

Dougherty, J.J., Wu, J. & Nichols, R.A. (2003) *β*-amyloid regulation of presynaptic nicotinic receptors in rat hippocampus and neocortex. *J. Neurosci.*, **23**, 6740–6747.

Gray, R., Rajan, A.S., Radcliffe, K.A., Yakehiro, M. & Dani, J.A. (1996) Hippocampal synaptic transmission enhanced by low concentrations of nicotine. *Nature*, **383**, 713–716.

Han, H.Q., Nichols, R.A., Rubin, M., Bähler, M. & Greengard, P. (1991) Induction of formation of presynaptic terminals in neuroblastoma cells by synapsin IIB. *Nature*, **349**, 697–700.

Kakio, A., Nishimoto, S.I., Yanagisawa, K., Kozutsumi, Y. & Matsuzaki, K. (2002) Interactions of amyloid β-protein with various ganglioside-bound form as an endogenous seed for Alzheimer amyloid. *Biochemistry*, **41**, 7385–7390.

La Magueresse, C. & Cherubini, E. (2007) Presynaptic calcium stores contribute to nicotine-elicited potentiation of evoked synaptic transmission at CA3-CA1 connections in the neonatal rat hippocampus. *Hippocampus*, **17**, 316–325.

Lee, D.H.S. & Wang, H.Y. (2003) Differential physiologic responses of α7 nicotinic acetylcholine receptors to β-amyloid$_{1\text{-}40}$ and β-amyloid$_{1\text{-}42}$. *J. Neurobiol.*, **55**, 25–30.

Liu, Q., Kawai, H. & Berg, D.K. (2001) β-Amyloid peptide blocks the response of α7-containing nicotinic receptors on hippocampal neurons. *Proc. Natl Acad. Sci. USA*, **98**, 4734–4739.

Liu, Q., Huang, Y., Xue, F., Simard, A., DeChon, J., Li, G., Zhang, J., Lucer, L., Wang, M., Sierks, M., Hu, G., Chang, Y., Lukas, R.J. & Wu, J. (2009) A novel nicotinic acetylcholine receptor subtype in basal forebrain cholinergic neurons with high sensitivity to amyloid peptides. *J. Neurosci.*, **29**, 918–929.

Lukyanetz, E.A., Piper, T.P. & Sihra, T.S. (1998) Calcineurin involvement in the regulation of high-threshold Ca^{2+} channels in NG108-15 (rodent neuroblastoma X glioma hybrid) cells. *J. Physiol.*, **510**, 371–385.

Mansvelder, H.D., Keath, J.R. & McGehee, D.S. (2002) Synaptic mechanisms underlie nicotine-induced excitability of brain reward areas. *Neuron*, **33**, 905–919.

McGee, R., Simpson, P., Christian, C., Mata, M., Nelson, P. & Nirenberg, M. (1978) Regulation of acetylcholine release from neuroblastoma X glioma hybrid cells. *Proc. Natl Acad. Sci. USA*, **75**, 1314–1318.

McGehee, D.S., Heath, M.J., Gelber, S., Devay, P. & Role, L.W. (1995) Nicotine enhancement of fast excitatory synaptic transmission in CNS by presynaptic receptors. *Science*, **269**, 1692–1696.

McLean, C.A., Cherny, R.A., Fraser, F.W., Fuller, S.J., Smith, M.J., Beyreuther, K., Bush, A.I. & Masters, C.L. (1999) Soluble pool of Aβ amyloid as a determinant of severity of neurodegeneration in Alzheimer's disease. *Ann. Neurol.*, **46**, 860–866.

Mehta, T.K., Dougherty, J.J., Wu, J., Choi, C.H., Khan, G.K. & Nichols, R.A. (2009) Defining presynaptic nicotinic receptors regulated by beta amyloid in mouse cortex and hippocampus with receptor null mutants. *J. Neurochem.*, **109**, 1452–1458.

Nagele, R.G., D'Andrea, M.R., Anderson, W.J. & Wang, H.Y. (2002) Intracellular accumulation of β-amyloid$_{1\text{-}42}$ in neurons is facilitated by the α7 nicotinic acetylcholine receptor in Alzheimer's disease. *Neuroscience*, **110**, 199–211.

Nayak, S.V., Rondé, P., Spier, A.D., Lummis, S.C.R. & Nichols, R.A. (2000) Nicotinic receptors co-localize with 5-HT3 serotonin receptors on striatal nerve terminals. *Neuropharmacology*, **39**, 2681–2690.

Nayak, S.V., Dougherty, J.J., McIntosh, J.M. & Nichols, R.A. (2001) Ca^{2+} changes induced by different presynaptic nicotinic receptors in separate populations of individual striatal nerve terminals. *J. Neurochem.*, **76**, 1860–1870.

Nelson, P., Christian, C. & Nirenberg, M. (1976) Synapse formation between clonal neuroblastoma X glioma hybrid cells and striated muscle cells. *Proc. Natl Acad. Sci. USA*, **73**, 123–127.

Nichols, R.A., Dengler, A.F., Nakagawa, E.M., Bashkin, M., Paul, B.T., Wu, J. & Khan, G.M. (2007) A constitutive, transient receptor potential-like Ca^{2+} influx pathway in presynaptic nerve endings independent of voltage-gated Ca^{2+} channels and Na^{+}/ Ca^{2+} exchange. *J. Biol. Chem.*, **282**, 36102–36111.

Pettit, D.L., Shao, Z. & Yakel, J.L. (2001) β-Amyloid$_{1\text{-}42}$ peptide directly modulates nicotinic receptors in the rat hippocampal slice. *J. Neurosci.*, **21**, RC120.

Puzzo, D., Privitera, L., Leznik, E., Fà, M., Staniszewski, A., Palmeri, A. & Arancio, O. (2008) Picomolar amyloid-β positively modulates synaptic plasticity and memory in hippocampus. *J. Neurosci.*, **28**, 14537–14545.

Role, L. & Berg, D.K. (1996) Nicotinic receptors in the development and modulation of CNS synapses. *Neuron*, **16**, 1077–1085.

Rondé, P. & Nichols, R.A. (2001) Postsynaptic target regulates functional responses induced by 5-HT$_3$ serotonin receptors on axonal varicosities of NG108-15 hybrid neuroblastoma cells. *Neuroscience*, **102**, 979–987.

Selkoe, D.J. (2002) Alzheimer's disease is a synaptic failure. *Science*, **298**, 789–791.

Selkoe, D.J. (2008) Soluble oligomers of the amyloid β-protein impair synaptic plasticity and behavior. *Behav. Brain Res.*, **192**, 106–113.

Selkoe, D.J. & Schenk, D. (2003) Alzheimer's disease: molecular understanding predicts amyloid-based therapeutics. *Annu. Rev. Pharmacol. Toxicol.*, **43**, 545–584.

Sharma, G. & Vijayaraghavan, S. (2003) Modulation of presynaptic store calcium induces release of glutamate and postsynaptic firing. *Neuron*, **38**, 929–939.

Sharma, G., Grybko, M. & Vijayaraghavan, S. (2008) Action potential-independent and nicotinic receptor-mediated concerted release of multiple quanta at hippocampal CA3-Mossy fiber synapses. *J. Neurosci.*, **28**, 2563–2575.

Small, D.H., Maksel, D., Kerr, M.L., Ng, J., Hou, X., Chu, C., Mehrani, H., Unabia, S., Azari, M.F., Loiacono, R., Aguilar, M.I. & Chebib, M. (2007) The β-amyloid protein of Alzheimer's disease binds to membrane lipids but does not bind to the α7 nicotinic acetylcholine receptor. *J. Neurochem.*, **101**, 1527–1538.

Tsui-Pierchala, B.A., Encinas, M., Millbrandt, J. & Johnson, E.M. (2002) Lipid rafts in neuronal signaling and function. *Trends Neurosci.*, **25**, 412–417.

Umbriaco, D., Watkins, K.C., Descarries, L., Cozzari, C. & Hartman, B.K. (1994) Ultrastructural and morphometric features of the acetylcholine innervation in adult rat parietal cortex: an electron microscopic study in serial sections. *J. Comp. Neurol.*, **348**, 351–373.

Walsh, D.M. & Selkoe, D.J. (2007) Aβ oligomers – a decade of discovery. *J. Neurochem.*, **101**, 1172–1184.

Wang, H.Y., Lee, D.H.S., D'Andrea, M.R., Peterson, P.A., Shank, R.P. & Reitz, A.B. (2000a) β-amyloid$_{1\text{-}42}$ binds to α7 nicotinic acetylcholine receptor with high affinity. *J. Biol. Chem.*, **275**, 5626–5632.

Wang, H.Y., Lee, D.H., Davis, C.B. & Shank, R.P. (2000b) Amyloid peptide A$\beta_{1\text{-}42}$ binds selectively and with picomolar affinity to α7 nicotinic acetylcholine receptors. *J. Neurochem.*, **75**, 1155–1161.

Wang, H.Y., Li, W., Benedetti, N.J. & Lee, D.H.S. (2003) α7 nicotinic acetylcholine receptors mediate β-amyloid peptide-induced tau protein phosphorylation. *J. Biol. Chem.*, **278**, 31547–31553.

Wang, H.Y., Stucky, A., Liu, J., Shen, C., Trocme-Thibierge, C. & Morain, P. (2009) Dissociating β-amyloid from α7 nicotinic acetylcholine receptor by a novel therapeutic agent, S 24795, normalizes α7 nicotinic acetylcholine and NMDA receptor function in Alzheimer's disease brain. *J. Neurosci.*, **29**, 10961–10973.

Warnock, D.E., Roberts, C., Lutz, M.S., Blackburn, W.A., Young, W.W. & Baeziger, J.U. (1993) Determination of plasma membrane lipid mass and composition in cultured Chinese hamster ovary cells using high gradient magnetic affinity chromatography. *J. Biol. Chem.*, **268**, 10145–10153.

Wu, J., Kuo, Y.P., George, A.A., Xu, L., Hu, L. & Lukas, R.J. (2004) β-amyloid directly inhibits human $\alpha 4\beta 2$-nicotinic acetylcholine receptors heterologously expressed in hum SH-EP1 cells. *J. Biol. Chem.*, **279**, 37842–37851.

Wu, J., Khan, G.M. & Nichols, R.A. (2007) Dopamine release in prefrontal cortex in response to β-amyloid activation of α7 * nicotinic receptors. *Brain Res.*, **1182**, 82–89.

Yakel, J.L., Shao, X.M. & Jackson, M.B. (1991) Activation and desensitization of the 5-HT$_3$ receptor in a rat glioma X mouse neuroblastoma hybrid cell. *J. Physiol.*, **436**, 293–308.

Zidovetzki, R. & Levitan, I. (2007) Use of cyclodextrins to manipulate membrane cholesterol: evidence, misconceptions and control strategies. *Biochem. Biophys. Acta*, **1768**, 1311–1324.